Distributed cooperative synchronization strategy for multi-bus microgrids

Sun, Yao; Zhong, Chaolu; Hou, Xiaochao; Yang, Jian; Han, Hua; Guerrero, Josep M.

Published in:
International Journal of Electrical Power & Energy Systems

DOI (link to publication from Publisher):
10.1016/j.ijepes.2016.09.002

Publication date:
2017

Document Version
Early version, also known as pre-print

Distributed Cooperative Synchronization Strategy for Multi-Bus Microgrids

Yao Sun[a], Chaolu Zhong[a], Xiaochao Hou[a,*], Jian Yang[a], Hua Han[a], Josep M. Guerrero[b] [a]Central South University, School of Information Science and Engineering, Changsha

[b]Aalborg University, Department of Energy Technology, Denmark joz@et.aau.dk

www.microgrids.et.aau.dk

* Corresponding author. Tel.: +86 15388034698; fax: +86 88 876 070.
E-mail address: houxc10@csu.edu.cn (X. Hou).

***Abstract*—Microgrids can operate in both grid-connected mode and islanded mode. In order to smooth transfer from islanded mode to grid-connected mode, it is necessary to synchronize the point of common coupling (PCC) with main utility grid (UG) in voltage frequency, phase and amplitude. Conventional synchronization methods based on centralized communication are very costly and not suitable for multi-bus microgrids that have a large number of distributed generators (DGs). To address this concern, this study presents an active synchronization control strategy based on distributed cooperation technology for multi-bus microgrids. The proposed method can reconnect the microgrid in island to UG seamlessly with sparse communication channels. Synchronization correction signals are generated by a voltage controller, which are only transmitted to the leader DGs. Meanwhile, each DG exchanges information with its neighbors. Finally, the voltage of PCC will synchronize with the main grid and all DGs will achieve the consensus behaviors. Compared with traditional synchronization methods, the proposed method does not need complex communication networks and improves flexibility and redundancy. Even if the distributed communication breaks down, the primary droop control can still operate robustly. Small signal model of entire system is developed to adjust the parameters of distributed active synchronization controller. Simulation results are presented to verify the effectiveness of the proposed method.**

***Keywords*--Active synchronization, distributed cooperation, droop control, networked microgrid, seamless transition.**

I. INTRODUCTION

AS an effective carrier of distributed power system, microgrids consist of various distributed energy sources, storages, power conversion devices, protections and load monitor equipment [1]-[2]. Typically, a microgrid is a local distributed electrical network which can operate in both grid-connected and islanded modes [3]. In grid-connected mode, the voltage and frequency are supported by the utility grid (UG), and all distributed generators (DGs) are controlled as controlled current sources. In islanded mode, DGs are required to participant into power sharing and voltage/frequency regulation. Thus, the DGs function as controlled voltage sources [4]-[5].

To guarantee uninterruptible and reliable power supplies, microgrids should offer a seamless transition between the two operation modes [6]-[7]. From the grid-connected mode to the islanded mode, the universal control strategies should be implemented to ensure smooth transition without any reconfiguration of control structure [8]. It is dangerous for a microgrid to be reconnected to utility grid in asynchronous states, because the voltage difference across the static switch would result in large inrush currents. Thus, pre-synchronization is necessary to achieve a smooth reconnection.

In the past researches, the main methods can be divided into two categories, either synchronizing one DG with the UG [9]-[10] or reconnecting microgrids to UG with a central controller [13]-[15], [19]-[22]. A single DG can be simply reconnected to the UG by the traditional synchronizer [9]-[10]. However, synchronizing a networked microgrid, where various DGs are dispersedly connected with their neighbors, is a greater challenge [11]-[12].

The central controller can make micogrids with multiple DGs resynchronize to the utility grid based on high bandwidth communications. In [13], an active synchronizing control strategy is proposed which involves a network-based coordinated control of multiple DGs. This scheme allows the microgrid synchronization under various operating conditions of DGs and loads change. However, it does not achieve a fast and optimized synchronization. In [14], a synchronization method for an islanded microgrid with two hydro generators is proposed. This method utilizes remote sensing of voltage with the help of communications. Small frequency mismatch between UG and PCC is directly added in the control loop, which delays the synchronization process and leads to reclosing time indefinite.

A phase locked loop (PLL)-based pre-synchronization control approach is presented in [15], where three different PLL structures are combined to synchronize the phase and frequency for all DGs. A common timing reference needs to be generated by the 1 pulse per second signal, provided by GPS devices [16]-[18], so the practicability of the method is weakened. These methods synchronize the frequency and phase in sequence, so the synchronization time is prolonged.

Alternatively, a self-synchronized method without dedicated PLL unit is proposed in [19], where virtual synchronization can automatically synchronize itself with UG. However, the method needs high bandwidth communication to collect instantaneous grid voltage and only operate without any local loads. On the whole, the central controller makes a control decision and then broadcasts the decision to each DG

[13]-[15], [19]-[22]. It requires much more and longer communication infrastructures, and such architecture is vulnerable to communication failures. Therefore, centralized control is impractical for wide networks populated by a number of DGs.

To enhance the system reliability and lower the investment in communications, the distributed control is a preferable method with only a sparse communication network. Thus, the system is less sensitive to failures and error modelling. It has features of scalability, robustness, and plug-and-play capability. Distributed control has been promoted by the increasing interest in networked multi-agent systems and many applications in smart grids [23]-[24]. *J. Simpson* and *F. Dorfler* propose the distributed-averaging integral controller to dynamically regulate the system frequency and preserve the power sharing properties [25]. Then, the averaging-based distributed controllers are extended to economic dispatch problem in one-to-one correspondence with the set of steady-states [26]. Moreover, distributed control strategies have been widely proposed for accurate power sharing and voltage/frequency recovery [27]-[30], and cost optimization [31]-[32] in microgrids. A general distributed scheme in [28] requires each local controller communicating with all the other controllers, which increases the communication cost. In [29], the voltage and frequency controller designs are separated. The distributed finite-time approach is used in voltage restoration and a consensus-based distributed frequency control is proposed for frequency restoration. In addition, for the identification of large-scale distributed control strategies, *J. Wei and D. Kundur* present a hierarchical cyber-physical multi-agent model of smart grid system operation based on flocking theory [33]-[35]. The appropriate degree of dependence on cyber information is determined to improve smart grid resilience and transient stability.

In order to overcome the drawbacks of the traditional centralized controller, this study firstly applies the distributed cooperation control to active synchronization strategy for multi-bus microgrids. The proposed method combines the primary droop control, distributed cooperation technology and active synchronization strategy. The focus of this study is the engineering application-oriented of the distributed active synchronization strategy and the system stability analysis for the multi-bus microgrids. Compared to existing approaches, the advantages are concluded as: 1) microgrid can be reconnected to UG seamlessly with sparse communication channels from islanded mode to grid-connected mode; 2) the voltage of grid connection point is dominated by the leader DGs, so the time of pre-synchronization isn't restricted by complex microgrid topology; 3) The cyber constraints are provided to guarantee the system stability and improve the system reliability; 4) with this method, the power sharing can be maintained in synchronization process; 5) the proposed method can be extended to grid-connected mode, which reaches a universal control to address different modes of operation.

The rest of this paper is organized as follows. In section II, the system structure and primary control are described. The proposed distributed cooperative synchronization strategy is presented in section III. Principles of selecting leader DG and microgrid synchronization criteria are discussed in section IV. In section V, system stability is analyzed to adjust the parameters of distributed active synchronization controller. In section VI, simulation results are provided. Finally, the conclusion follows in Section VII.

II. The System Structure and Primary Control of DGs

A. Critical Issue Description of Active Synchronization for Multi-Bus Microgrids

The system structure of a multi-bus microgrid contains *n* buses, DGs, transmission lines, loads, synchronous controller and communication links as shown in Fig. 1. The point of common coupling (PCC) in the microgrid is connected to the UG through a static switch. v_g and v_c represent the voltage of UG and PCC, respectively. The synchronous controller is used to generate synchronization correction signals $\Delta\omega^*_{syn}$ and ΔV^*_{syn} by the voltage differences between the PCC and UG.

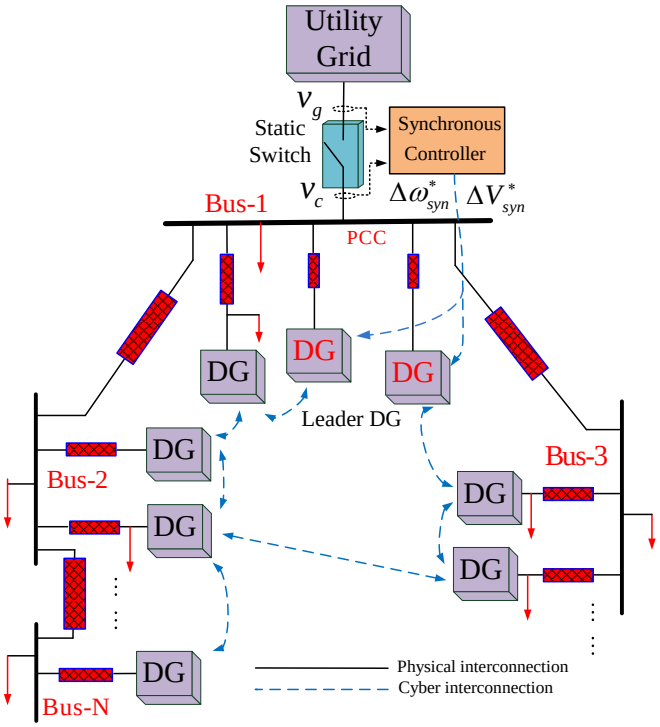

Fig. 1. The structure of microgrid with distributed sparse communication.

If the microgrid reconnects to the grid without a proper active synchronization strategy, the voltage differences between v_c and v_g would result in large inrush currents. It is dangerous for microgrid operations. To decrease the large inrush currents and ensure the uninterrupted operation of critical loads, the grid synchronization method is very crucial. To achieve a smooth and successful reconnection, v_c must be synchronized with v_g in voltage phase, frequency and amplitude. Thus, the DGs should cooperate to adjust their

voltage and frequency to eliminate the differences between v_c and v_g.

In existing methods, the central control is the main method through a star communication network. The correction signals $\Delta\omega^*_{syn}$ and ΔV^*_{syn} are added to the frequency and voltage amplitude references of each DG by high bandwidth communications [15]. However, this communication structure poses a challenge in the multi-bus microgrid.

To overcome the drawbacks of the central control method, this paper adopts the distributed control to resynchronize microgrid with UG. With the distributed control, the synchronization correction signals $\Delta\omega^*_{syn}$ and ΔV^*_{syn} are only sent to the leader DG(s). The leader DG(s) will share its output frequency and reactive power to its neighbors. In addition, each DG only requires its own and adjacent information to adjust the voltage of PCC. When the consensus is achieved, all DGs would follow the leader DG(s) and main grid. The proposed method only needs sparse communication channels and is less sensitive to the failure of communication links. So, the system flexibility and reliability are improved.

B. Primary Droop Control of Microgrid in Islanded Mode

In the islanded mode, two main control objectives of the microgrid are to share the load demand among multiple parallel connected inverters proportionately and to maintain the stability of voltage and frequency [3]. The droop control law for frequency and voltage are expressed as follows

$$\begin{cases} \omega_i = \omega^* - m_i P_i \\ V_i = V^* - n_i Q_i \end{cases} \tag{1}$$

where ω^* and V^* indicate the reference values for the angular frequency and amplitude of inverter output voltage at no load, P_i and Q_i are the output active and reactive power of the i-th DG. m_i and n_i are the P-ω and Q-V droop coefficients of the i-th DG, respectively.

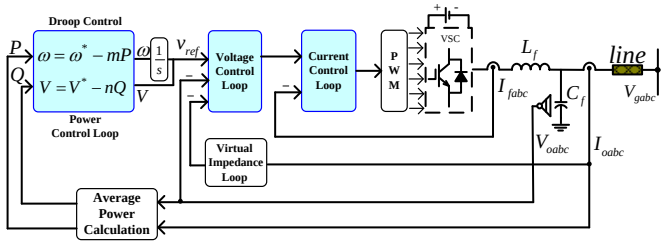

Fig. 2. The control scheme of inverter-based DG.

Microgrids consist of a cluster of loads and DGs, whose inter-connections are commonly power electronic converters [3]. Unlike the synchronous generator in the conventional power system, the inverter-based DGs have inherent features: fast response, less-inertia and weak overload capacity. The inner dynamics of inverter-based DGs could be ignored, which is always treated as a controlled voltage sources.

Fig. 2 shows a classic control scheme of an inverter-based DG. The control involves two layers: a power control layer and a double closed-loop layer for voltages and currents of the inverter. Usually, the virtual impedance is utilized for decoupling P/Q when the line impedance is mixed resistive and inductive [4].

III. Proposed Distributed Active Synchronization Control Strategy

The grid synchronization, which prepares islanded microgrid for grid connection, is a critical procedure of the entire operation [36]. This study aims at reconnecting the multi-bus microgrid back to the utility grid seamlessly after islanding. The proposed method allows multiple droop-controlled DGs to adjust the frequency, phase and amplitude to prepare for reconnecting the microgrid back to utility grid.

A. Synchronization correction signals

The goal of grid synchronization is to eliminate the voltage errors between UG and PCC. In a three-phase microgrid, the error of the voltage phase angle is calculated by the cross product of voltage vectors between PCC and UG as follows

$$\begin{aligned} e_\theta &= V_c V_g \sin(\theta_g - \theta_c) \\ &= -v_{g\alpha} v_{c\beta} + v_{g\beta} v_{c\alpha} \end{aligned} \tag{2}$$

where $v_{g\alpha}$ and $v_{c\alpha}$ are voltage components of utility grid and PCC on direct axis; $v_{g\beta}$ and $v_{c\beta}$ are voltage components on quadrature axis.

From (2), e_θ is identically equal to zero forever only when both angular frequency difference and angle difference are zero.

The error of the voltage amplitude is expressed as

$$e_U = V_g - V_c = \sqrt{v_{g\alpha}^2 + v_{g\beta}^2} - \sqrt{v_{c\alpha}^2 + v_{c\beta}^2} \tag{3}$$

Then, e_θ and e_U are fed back to a proportional integration (PI) controller to generate synchronization correction signals, which are only sent to the leader distributed generators (DGs). Therefore, the angular frequency difference, angle difference and amplitude difference are zero when v_c would synchronize with v_g .The synchronization correction signals $\Delta\omega^*_{syn}$ and ΔV^*_{syn} are expressed as

$$\Delta\omega^*_{syn} = (k_{ps} + \frac{k_{is}}{s})(\frac{-v_{g\alpha} v_{c\beta} + v_{g\beta} v_{c\alpha}}{V_c V_g}) \tag{4}$$

$$\Delta V^*_{syn} = (k_{pvs} + \frac{k_{ivs}}{s})\left(\sqrt{v_{g\alpha}^2 + v_{g\beta}^2} - \sqrt{v_{c\alpha}^2 + v_{c\beta}^2}\right) \tag{5}$$

where k_{ps} , k_{pvs} are the proportional coefficients and k_{is} , k_{ivs} are integration coefficients.

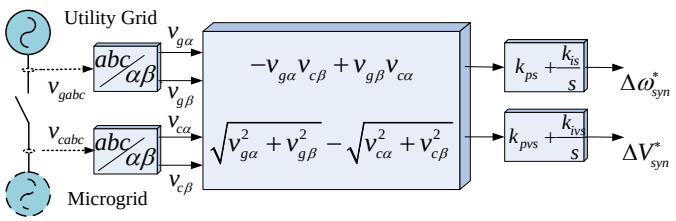

Fig. 3. Synchronization correction signals generation.

B. Distributed Frequency and Phase Synchronization

The concepts of cooperative and multi-agent control were initially inspired by the synchronization phenomena observed in the nature, where each agent only exchanges information with neighbor agents according to a prescribed communication graph [37]-[39]. The objective is to develop local decisions and control protocols that do not rely on a central authority, yet result in attestable accomplishment of global performance goals [37]. The cooperative schemes fall into two main categories, consensus problem and tracking problem [38]-[39]. In an islanded microgrid, all DGs have the same constant steady-state values, known as the cooperation consensus problem. But, in pre-synchronization process, as leader nodes must follow the main grid, the active synchronization is a tracking problem.

Graph theory is often used to describe the communication topology in microgrids [27]. Each DG is regarded as one node of the communication digraph. The communication layer is described by a weighted graph $G(\nu,\varepsilon,A)$ where $\nu=\{1,2,\cdots,n\}$ is a non-empty finite set for n DGs, $\varepsilon\subseteq\nu\times\nu$ is the prescribed communication links, and $A=[a_{ij}]\in R\times R$ is the associated adjacency matrix. In this paper, if there is an edge from node ν_j to node ν_i, then $a_{ij}=1$. As the communication is bi-directional, $a_{ij}=a_{ji}$. When all DGs are connected with the distributed communication, it should be noted that matrix $A=[a_{ij}]\neq 0$.

For the DG-*i*, the frequency regulation with distributed cooperation control is proposed as

$$\omega_i=\omega^*-m_iP_i+\Delta\omega_i \tag{6}$$

$$k_w\frac{d\Delta\omega_i}{dt}=\sum_{j\in N,\,j\neq i}a_{ij}(\Delta\omega_j-\Delta\omega_i)+\gamma_i(\Delta\omega_{syn}^*-\Delta\omega_i) \tag{7}$$

where $\Delta\omega_i$ is additional control variable, which will be equal to $\Delta\omega_{syn}^*$ in steady state. k_ω is a positive gain. If the DG-*i* is a leader DG, then $\gamma_i=1$; Otherwise, $\gamma_i=0$.

Fig. 4 depicts the primary P-ω droop control before and after the distributed control. One can interpret the distributed control action as a uniform shifting of all DGs to the utility grid angular frequency ω_g.

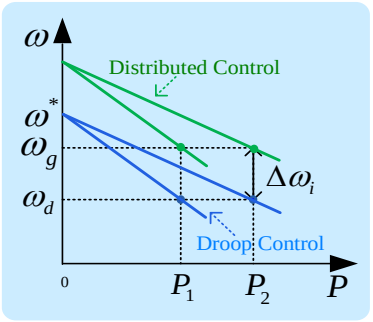

Fig. 4. P-ω droop control before and after the distributed control.

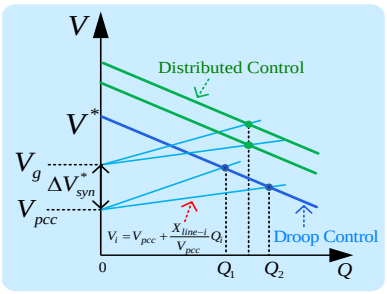

Fig. 5. Q-V droop control before and after the distributed control.

C. Distributed Voltage Regulation and Reactive Power Sharing

The voltage regulation of the active synchronization strategy is proposed as follows

$$V_i=V^*-n_iQ_i+\Delta V_i+\beta_i\Delta V_{syn}^* \tag{8a}$$

$$k_v\frac{d\Delta V_i}{dt}=\sum_{j\in N,\,j\neq i}b_{ij}(k_{Qj}Q_j-k_{Qi}Q_i) \tag{8b}$$

where β_i is the gain of voltage synchronization correction ΔV_{syn}^*. k_v is a positive gain. For the leader DGs, $\beta_k=1$ and $b_{kj}=0$. While for all other DGs, $\beta_i=0$ and $b_{ij}=1$. That is to say, only the leader DG-*k* regulates the PCC voltage to the voltage of main grid, and the follower DGs are controlled to share reactive power in a manner consistent with the voltage regulation of DG-*k*. Fig. 5 depicts Q-V droop control and reactive power sharing for two parallel DGs. As line impedances $X_{line-1}>X_{line-2}$, reactive power sharing cannot be shared by primary droop control. Under the distributed control, both the reactive power sharing and the voltage amplitude synchronization with the utility grid voltage could be achieved.

Fig. 6 shows the overall control block diagram of active synchronization strategy with some details. The cyber layer comprises all communication links and this is a sparse communication network, such that in case of any link failure the remaining network still contains a spanning tree. The correction signals, $\Delta\omega_{syn}^*$ and ΔV_{syn}^* only send to the leader DGs. The leader DGs regulates the voltage of PCC with the coordination of all other follower DGs. The "leader-follower" relationship among the DGs is set up to form a cluster around the voltage value of $v_c=v_g$. For all DGs, the droop control functions as the primary control to enhance system robustness. But the voltage deviation and mismatch of reactive power sharing cannot be overcome. Additionally, the distributed cooperation control can also be utilized to compensate the disadvantages of droop control in power sharing and voltage-frequency recovery.

IV. Principles of Selecting Leader DG(s) and Synchronization Criteria

A. Principles of Selecting Leader DG(s)

Only the leader DG(s) receives the synchronization correction signals from the synchronous controller, so

selecting proper leader DG(s) is pivotal in accordance with associated principles. For the parallel DGs and other buses at the grid connection bus in Fig. 7, the voltage amplitude, phase and frequency of PCC can be deduced.

According to Millman's theorem [40], the voltage phasor $\mathbf{v_c}$ of PCC can be given by

$$\mathbf{v_c} = \left(\frac{X_{prll}}{X_1}\right)\mathbf{v_1} + \left(\frac{X_{prll}}{X_2}\right)\mathbf{v_2} + \cdots + \left(\frac{X_{prll}}{X_n}\right)\mathbf{v_n} \tag{9}$$

where $\mathbf{v_n}$ is the voltage phasor of n-th DG or bus, X_n is the line reactance between each DG or bus and the common grid bus. For simplicity, the line resistance is neglected. X_{prll} is the equivalent parallel reactance, which is solved as

$$\frac{1}{X_{prll}} = \frac{1}{X_1} + \frac{1}{X_2} + \cdots + \frac{1}{X_n} \tag{10}$$

Rewriting (9) in the form with real and imaginary parts

$$\begin{aligned} V_c(\cos\delta_c + j\sin\delta_c) = c_1V_1(\cos\delta_1 + j\sin\delta_1) + \cdots \\ + c_nV_n(\cos\delta_n + j\sin\delta_n) \end{aligned} \tag{11}$$

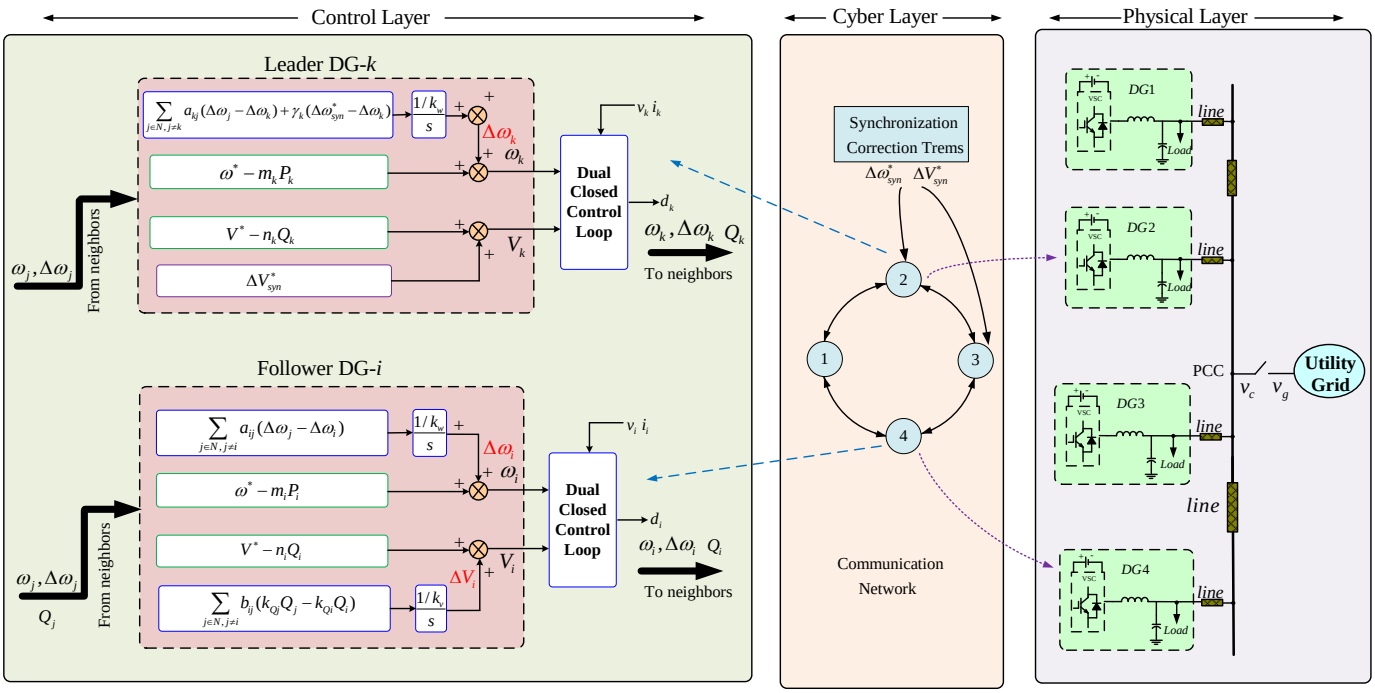

Fig. 6. Block diagram of active synchronization control strategy for leader DG-k and follower DG-i.

where

$$c_n = \frac{X_{prll}}{X_n} \geq 0\ ; \qquad \sum c_n = 1 \tag{12}$$

Actually, the power angle between the DG/bus and PCC is small, and the angle of PCC is regarded as phase angle reference [4].

$$\begin{cases} \cos\delta_k = 1 \\ \sin\delta_k = \delta_k \end{cases} \quad \forall k \in 1,2,\cdots,n \tag{13}$$

Substituting (13) into (11) yields

$$V_c(1+j\delta_c) = c_1V_1(1+j\delta_1) + \cdots + c_nv_n(1+j\delta_n) \tag{14}$$

The real parts of both sides in (14) must be equal. Then, the voltage amplitude of PCC can be obtained as

$$V_c = c_1V_1 + c_2V_2 \cdots + c_nV_n \tag{15}$$

When the output voltage of DGs changes, the relationship of various voltage change rates can be given by

$$\Delta V_c = c_1\Delta V_1 + c_2\Delta V_2 \cdots + c_n\Delta V_n \tag{16}$$

The imaginary parts of both sides in (14) must also be equal. Then, the phase angle of PCC can be obtained as

$$\delta_c = d_1\delta_1 + d_2\delta_2 \cdots + d_n\delta_n \tag{17}$$

where

$$d_n = \frac{V_n}{V_c}c_n\ ; \qquad \sum d_n = 1 \tag{18}$$

As the output voltage V_n of DG is approximately equal to V_c of PCC, d_n mostly depends on c_n. When the power transmission changes between the DG and PCC, the change value of phase angle is presented as

$$\Delta\delta_c = d_1\Delta\delta_1 + d_2\Delta\delta_2 \cdots + d_n\Delta\delta_n \tag{19}$$

Differentiating (19) yields

$$\Delta\omega_c = d_1\Delta\omega_1 + d_2\Delta\omega_2 \cdots + d_n\Delta\omega_n \tag{20}$$

From (16), (19) and (20), the voltage amplitude, phase and frequency change rates of PCC are the weighted average of all DGs. Weighting factors are dependent on the line inductances. Therefore, the DGs with higher rated power capacity should be installed closely to PCC, which function as leader DGs. In this sense, the leader DGs have a higher weightage in determining the PCC characteristics.

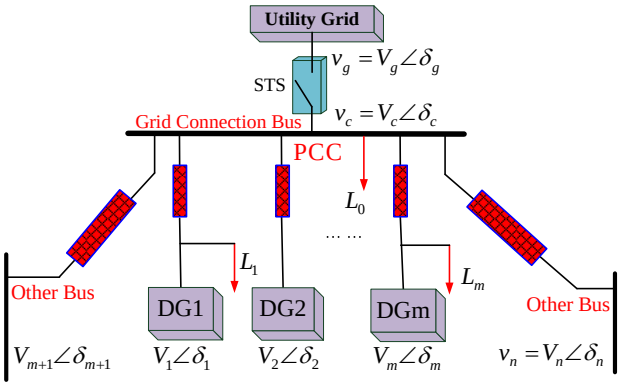

Fig. 7. The Structure of parallel local DGs or other buses at the grid connection bus of PCC (*m* DGs and *n*-*m* Buses).

B. Cyber Constraints

1) Number Constraint of Leader DGs

Leader DG(s) receives the synchronization correction signals from the synchronous controller. The greater the number of leader DGs installed in the multi-bus microgrid, the higher speed of pre-synchronization process. However, the associated investment would be increased. There is an inherent tradeoff between the time of pre-synchronization and the communication complexity. In this study, to guarantee the normal system operation when one leader DG fails, the microgrid should contain at least two leader DGs.

$$\sum_{i=1}^{n}\gamma_i \geq 2 \tag{21}$$

2) Distributed Communication Network Constraint

In this study, if there is a communication connection from DG-*j* to DG-*i*, we assume $a_{ij}=1$. As the communication is bi-directional, $a_{ij}=a_{ji}$. When all DGs are connected with the distributed communication, there should be a spanning tree to maintain the system stability. Thus, the adjacency matrix A should meet the requirement as follows

$$A=[a_{ij}]_{n\times n}\neq 0 \tag{22}$$

3) Cyber Interconnection Constraint for Each DG

To improve the system reliability and overcome the failure of single point, there should be no less than two direct/indirect communication path from each DG to leader DG. Thus, the system possesses high resilience to one communication link failure. The cyber constraints for each DG are given by

$$\sum_{j=1}^{n}a_{ij}\geq 2 \quad \text{and} \quad \sum_{i=1}^{n}a_{ij}\geq 2 \tag{23}$$

C. The synchronization Criteria

Once the synchronization criterion is met, the synchronous controller will send a command to close static switch during the pre-synchronization process. According to the synchronization criteria of IEEE Standard 1547-2003 [41], the microgrid should meet the synchronization criterion listed in Table I. However, the inverter-based DGs have the features: fast response, low-inertia and weak overload capacity. To avoid large inrush current and achieve a smooth and successful reconnection, the existing criteria in Table I should be replaced by more rigid criteria [11], [13], [42]. The adopted synchronization criterion is illustrated in Fig. 8.

TABLE I
DG Synchronization Criteria of IEEE Standard 1547-2003

Aggregate rating of DG (kVA)	*Frequency difference (HZ)*	*Voltage difference(%)*	*Phase angle difference (°)*
0-500	0.3	10	20
>500-1500	0.2	5	15
>1500-10000	0.1	3	10

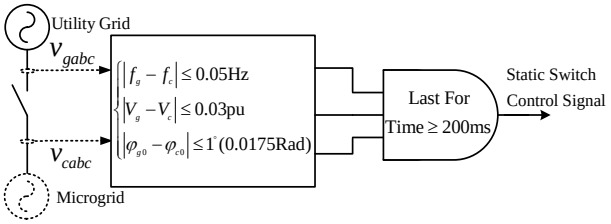

Fig. 8. Microgrid synchronization criteria for 0-500kVA rated capacity.

V. Stability Analysis

To analyze the system stability and adjust the parameters of distributed active synchronization controller, a small signal model has been developed according to the studied microgrid as shown in Fig.7.

A. Overall System Model

For the multiple parallel DGs and buses connected to the PCC, their dynamic control laws are presented as follows from (6a)-(7a)

$$\begin{cases}\dot{\delta}_1=\omega^*-m_1P_1+\Delta\omega_1\\ \dot{\delta}_2=\omega^*-m_2P_2+\Delta\omega_2\\ \vdots\\ \dot{\delta}_n=\omega^*-m_nP_n+\Delta\omega_n\end{cases} \tag{24}$$

where

$$\dot{\delta}_i=\omega_i \qquad (i=1,2\cdots n) \tag{25}$$

$$P_i=\frac{V_iV_c}{X_i}\sin\left(\delta_i-\delta_c\right) \tag{26}$$

where V_i and δ_i are the voltage magnitude and angle of the *i*-th DG/bus, respectively. V_c and δ_c are the voltage magnitude and angle of the grid connection bus, respectively. X_i is the line reactance between each DG/bus and the common grid bus.

As aforementioned, the outputs $\Delta\omega_i$ of the distributed cooperation control obtained through (6)-(7) are added to the droops to reconnect the islanded microgrid to utility grid seamlessly.

$$\begin{cases} \Delta\omega_1 = \frac{1}{k_\omega}\int\sum a_{1i}\left(\Delta\omega_i - \Delta\omega_1\right)dt + \frac{1}{k_\omega}\int\gamma_1\left(\Delta\omega_{syn}^* - \Delta\omega_1\right)dt \\ \Delta\omega_2 = \frac{1}{k_\omega}\int\sum a_{2i}\left(\Delta\omega_i - \Delta\omega_2\right)dt + \frac{1}{k_\omega}\int\gamma_2\left(\Delta\omega_{syn}^* - \Delta\omega_2\right)dt \\ \vdots \\ \Delta\omega_n = \frac{1}{k_\omega}\int\sum a_{ni}\left(\Delta\omega_i - \Delta\omega_n\right)dt + \frac{1}{k_\omega}\int\gamma_n\left(\Delta\omega_{syn}^* - \Delta\omega_n\right)dt \end{cases} \quad (27)$$

where $\Delta\omega_{syn}^*$ presents the synchronization correction signal, expressed as follows in the synchronization controller (2), (4)

$$\Delta\omega_{syn}^* = k_{ps}\sin\left(\omega_g t - \delta_c\right) + k_{is}\int\sin\left(\omega_g t - \delta_c\right)dt \quad (28)$$

where ω_g is the angular frequency of the utility grid.

Moreover, according to the system constraints, the supply-demand power must be balanced. The equivalent equation is described

$$P_1 + P_2 + \cdots + P_n = P_L \quad (29)$$

where P_L presents a value of the total load power demand.

B. Model Linearization

Assume that the power angle $|\delta_n - \delta_c|_\infty$ is always small, and then the linearization of the system model is derived.

1) Primary Control Strategy Linearization of (24)

$$\dot{\tilde{\delta}} = -K\left(\tilde{\delta} - \tilde{\delta}_c\eta\right) + \Delta\tilde{\omega} \quad (30)$$

where

$$\begin{cases} \tilde{\delta} = \begin{bmatrix}\tilde{\delta}_1 & \tilde{\delta}_2 & \cdots & \tilde{\delta}_n\end{bmatrix}^T \\ \eta = \begin{bmatrix}1 & 1 & \cdots & 1\end{bmatrix}^T \\ \Delta\tilde{\omega} = \begin{bmatrix}\Delta\tilde{\omega}_1 & \Delta\tilde{\omega}_2 & \cdots & \Delta\tilde{\omega}_n\end{bmatrix}^T \\ K = \begin{bmatrix} m_1k_1 & & & \\ & m_2k_2 & & \\ & & \ddots & \\ & & & m_nk_n \end{bmatrix} \\ k_n = \frac{V_nV_c}{X_n}\cos\left(\delta_n - \delta_c\right) \end{cases} \quad (31)$$

2) Distributed Cooperation Control Linearization of (27)

$$\Delta\dot{\tilde{\omega}} = -L\Delta\tilde{\omega} + \gamma\left(\Delta\tilde{\omega}_{syn}^*\eta - \Delta\tilde{\omega}\right) \quad (32)$$

where

$$\begin{cases} L = \frac{1}{k_\omega}\begin{bmatrix} \sum a_{1i} & -a_{12} & \cdots & -a_{1n} \\ -a_{21} & \sum a_{2i} & \cdots & -a_{2n} \\ \vdots & \vdots & \ddots & \vdots \\ -a_{n1} & -a_{n2} & \cdots & \sum a_{ni} \end{bmatrix} \\ \gamma = \frac{1}{k_\omega}\begin{bmatrix} \gamma_1 & & & \\ & \gamma_2 & & \\ & & \ddots & \\ & & & \gamma_n \end{bmatrix} \end{cases} \quad (33)$$

3) Active synchronization Control Linearization of (28)

$$\Delta\dot{\tilde{\omega}}_{syn}^* = k_{ps}\left(\omega_g - \dot{\tilde{\delta}}_c\right) + k_{is}\left(\omega_g t - \tilde{\delta}_c\right) \quad (34)$$

4) System Constraint Linearization of (29)

$$k_1\left(\tilde{\delta}_1 - \tilde{\delta}_c\right) + \cdots + k_n\left(\tilde{\delta}_n - \tilde{\delta}_c\right) = 0 \quad (35)$$

5) Entire System Linearization

For the tracking problem of distributed active synchronization, a new state variable $\tilde{\theta}$ is chose to facilitate the system stability analysis.

$$\tilde{\theta} = \tilde{\delta} - (\omega_g t)\eta \quad (36)$$

Then, the entire system linearization is combined

$$\begin{cases} \dot{\tilde{\theta}} = -K_1\tilde{\theta} + \Delta\tilde{\omega} - \omega_g\eta \\ \Delta\dot{\tilde{\omega}} = -L\Delta\tilde{\omega} + \gamma\left(\Delta\tilde{\omega}_{syn}^*\eta - \Delta\tilde{\omega}\right) \\ \Delta\dot{\tilde{\omega}}_{syn}^* = \left(\frac{k_{ps}}{k_{tol}}K_2K_1 - \frac{k_{is}}{k_{tol}}K_2\right)\tilde{\theta} - \frac{k_{ps}}{k_{tol}}K_2\left(\Delta\tilde{\omega} - \omega_g\eta\right) \end{cases} \quad (37)$$

where

$$\begin{cases} k_{tol} = \sum_{i=1}^{n} k_i \\ K_2 = \begin{bmatrix}k_1 & k_2 & \cdots & k_n\end{bmatrix} \\ K_1 = K - \frac{1}{k_{tol}}\begin{bmatrix}m_1k_1 & m_2k_2 & \cdots & m_nk_n\end{bmatrix}^T\begin{bmatrix}k_1 & k_2 & \cdots & k_n\end{bmatrix} \end{cases} \quad (38)$$

To examine the stability of the system, the state-space equations must be manipulated to a system of the form

$$\dot{\tilde{X}} = [\mathrm{A}]\dot{\tilde{X}} \quad (39)$$

In this study, given

$$\tilde{X} = \begin{bmatrix} \tilde{\theta}_{1\times n} \\ \Delta\tilde{\omega}_{1\times n} \\ \Delta\tilde{\omega}_{syn}^* \end{bmatrix} \quad (40)$$

$$A = \left[\begin{array}{ccc|ccc|c} & & & & & & 0 \\ & -(K_1)_{n\times n} & & & I_{n\times n} & & \vdots \\ & & & & & & 0 \\ \hline & & & & & & \gamma_1 \\ & 0_{n\times n} & & & -(\mathrm{L}+\gamma)_{n\times n} & & \vdots \\ & & & & & & \gamma_n \\ \hline A_1 & \cdots & A_n & \frac{k_{ps}k_1}{k_{tol}} & \cdots & \frac{k_{ps}k_n}{k_{tol}} & 0 \end{array}\right] \quad (41)$$

where

$$A_n = \frac{k_n}{k_{tol}}\{k_{ps}[m_nk_n - \frac{\sum m_nk_n^2}{k_{tol}}] - k_{is}\} \quad (42)$$

C. Eigenvalue Analysis

The eigenvalues of matrix A can be used to study the stability of the system around the state of equilibrium. For the simulation system to be described later in Section VI, the root-locus plots of matrix A are shown in Fig. 9 while varying the parameters, k_{ps}, k_{is} and k_ω.

Fig. 9 reveals that the system is stable for all three cased. Firstly, with k_{ps} increases in Fig. 9(a), the dominant eigenvalues (λ_1 and λ_2) gradually move away from the real

axis. Meanwhile, the eigenvalue λ_3 moves close to the imaginary axis which decreases the damping ratio of the system.

Secondly, in Fig. 9(b), when k_{is} is small, λ_3 is the dominant eigenvalue, and several pairs of complex-conjugate roots are far from the imaginary axis. The system can be equivalent to a first order system without overshoot. However, when k_{ps} increases, λ_1 and λ_2 become dominant, obtaining a second-order behavior. In the meantime, λ_1 and λ_2 move close to the imaginary axis, which makes the system more easy to become unstable.

Thirdly, increasing k_ω attracts the complex conjugate poles (λ_1 and λ_2) to the real axis and imaginary axis, which may result in instability. Thus, the value of k_ω should not be designed too large.

VI. Simulation Results

The proposed distributed cooperative synchronization control strategy is verified with simulation carried out in Matlab/Simulink. The parameters used in simulation are listed in Table II. The phase locked loop (PLL) measurement unit is adopted to acquire the physical data of the inverter-based DG, including the voltage magnitude, angle and frequency in a discrete manner. Then, the output average power is calculated by the product of the instantaneous voltage and currents. The power control layer and a double closed-loop layer for an inverter-based DG are described in Fig. 2 in detail.

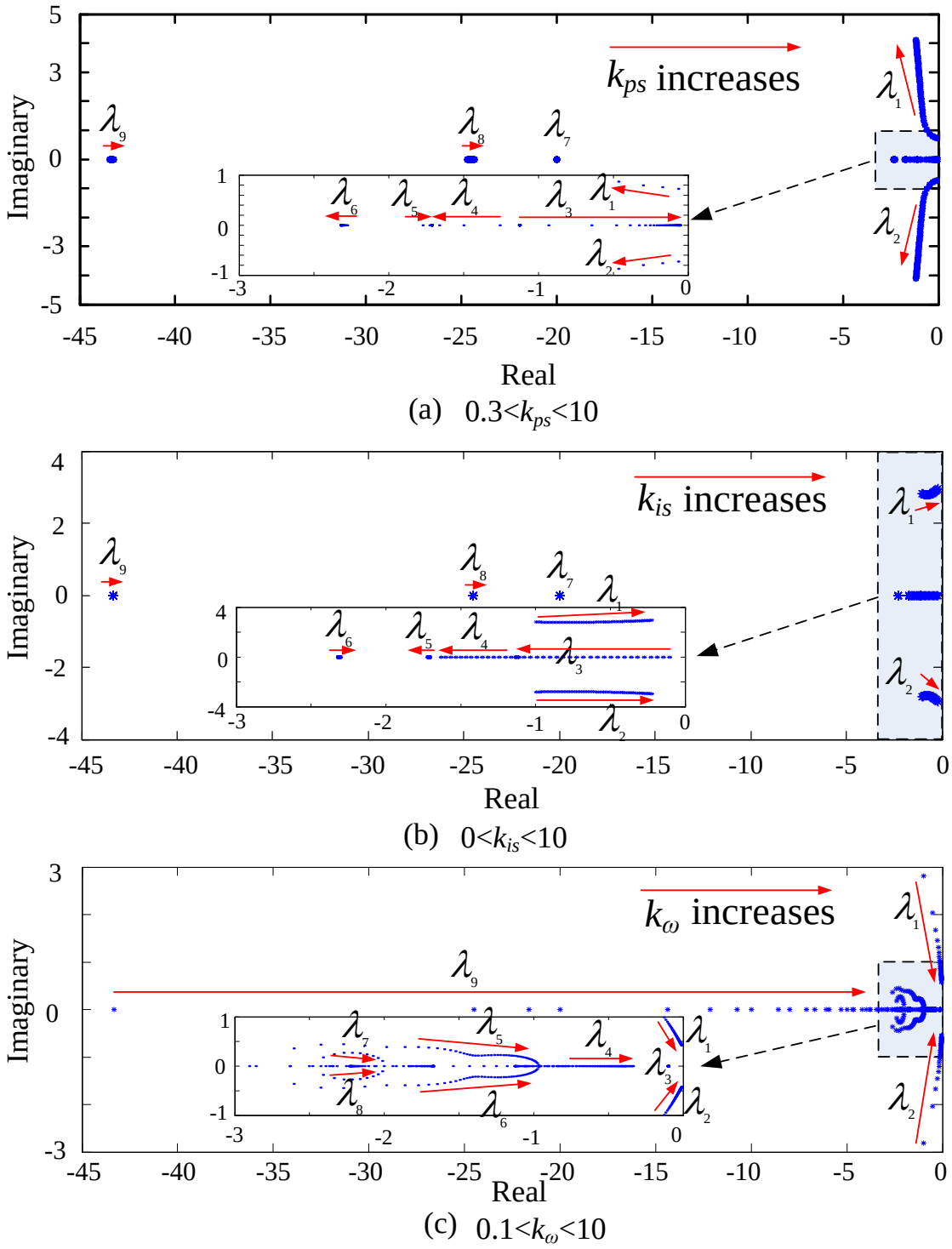

Fig. 9. Eigenvalues of system matrix A for the simulation model: (a) $0.3<k_{ps}<10$, (b) $0< k_{is}<10$, (c) $0.1< k_{\omega}<10$.

The simulated system model and communication cyber are shown in Fig. 10, where the microgrid consists of four DGs, four respective local loads and a common load. As the simulated microgrid model contains few DGs, only the DG1 is treated as the leader DG and receives synchronization correction signals from synchronous controller. All DGs communicate with its neighbors and the associated adjacency matrices $A=[a_{ij}]$ and $B=[b_{ij}]$ are presented as follows

$$A=\begin{pmatrix}0&1&0&1\\1&0&1&0\\0&1&0&1\\1&0&1&0\end{pmatrix},\quad B=\begin{pmatrix}0&1&0&1\\0&0&0&0\\0&1&0&1\\1&0&1&0\end{pmatrix} \tag{43}$$

A. Scenario I: Proposed Distributed Cooperative Synchronization Control Strategy

In this case, the proposed distributed cooperative synchronization control strategy is verified. It is assumed that

the microgrid is disconnected from main grid and operates in islanded mode at the beginning, and only droop is applied. The distributed cooperative synchronization control strategy is applied at $t = 1\text{s}$, and the static switch is closed when the frequency difference, phase angle difference, and amplitude difference of grid and PCC voltage meet the microgrid synchronization criterion. The simulation results are exhibited in Fig. 11.

TABLE II
Simulation Parameters

Parameter	*Symbol*	*Value*
Electrical parameters		
Nominal voltage	E	311V
Nominal frequency	f^*	50Hz
Line impedance	Z_{01}	$R = 0.8\Omega,\ L = 3\text{mH}$
Line impedance	Z_{02}	$R = 1.6\Omega,\ L = 6\text{mH}$
Line impedance	Z_{23}	$R = 0.9\Omega,\ L = 4\text{mH}$
Line impedance	Z_{04}	$R = 1.2\Omega,\ L = 5\text{mH}$
Load $L_1 = L_2 = L_3 = L_4$		$P = 10^3\text{W},\ Q = 10^3\text{Var}$
Load L_0		$P = 4\times10^3\text{W},\ Q = 3\times10^3\text{Var}$
Synchronous Controller Parameters		
Angle-frequency proportional term	k_{ps}	5
Angle-frequency integral term	k_{is}	0.5
Voltage proportional term	k_{pvs}	2
Voltage integral term	k_{ivs}	1
Droop Control Parameters		
Rated active power	P_{max}	10kW
Rated reactive power	Q_{max}	3kVar
P-w droop coefficient	m_i	$10^{-5}\text{rad}/(\text{W}\cdot\text{s})$
Q-V droop coefficient	n_i	$10^{-3}\text{V}/\text{Var}$
Distributed Cooperation Parameters		
Frequency gain	k_w	0.1
Voltage gain	k_v	0.01

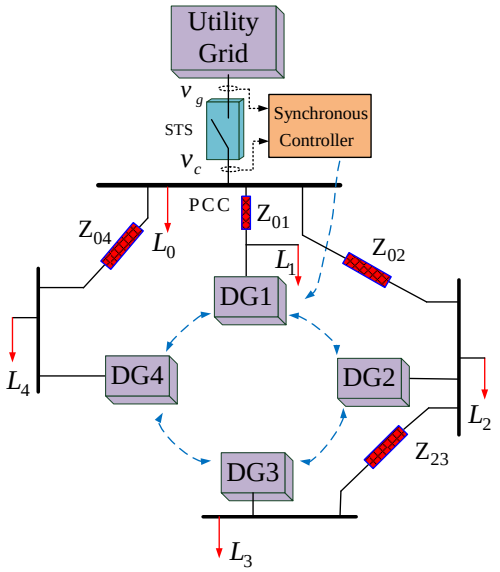

Fig. 10. Simulated microgrid model and communication cyber.

As shown from Fig. 11(d)-(h), when the proposed method is activated, the instantaneous voltage differences Δv of PCC and grid is gradually decreased. At the moment when the frequency, phase angle and amplitude of PCC meet the microgrid synchronization criteria at Fig. 8, the instantaneous voltage differences are almost zero, and the static switch is closed. The instantaneous grid currents are small and almost no inrush. A seamless synchronization is achieved. In addition, from Fig. 11(a)-(c), the proposed method can not only restore frequency and voltage of the MG but also ensure reactive power sharing.

B. Scenario II: Resiliency to communication link failure

In centralized active synchronization strategies, communication failures of one link will produce the fail down of the whole system, so star communication network reduces the system reliability. Alternatively, the distributed cyber can overcome the failure of single point and feature plug-play functionality. In this case, the communication link between DG units 2 and 3 fails to test the flexibility and redundancy of system. From (43), the associated adjacency matrix $A = [a_{ij}] \neq 0$ meets the distributed communication network constraint of (22). Simulation process is similar to Scenario I. As results in Fig. 12 show, the proposed method is still applicable. The grid current is so small that microgrid can be reconnected to main grid seamlessly. Only if there is also a direct/indirect communication path between each DG and leader DG after one link failure, the distributed coopertive synchronization method can reconnect microgrid back to UG effectively.

VII. Conclusion

This paper proposes a distributed active synchronization strategy for a networked microgrid, which can reconnect microgrid back to utility grid seamlessly with sparse communication channels. Leader and follower DGs are designed based on different geography locations and rated power capacity. Only leader DG receives synchronization correction signals from synchronous controller. The rest DGs will follow the leader DG through designed consensus protocol. Compared with traditional central controller, the proposed method reduces communications costs and improves flexibility and redundancy. Moreover, the distributed cooperation method can be extended to grid-connected mode and regarded as a universal control, which can address transition process of different modes.

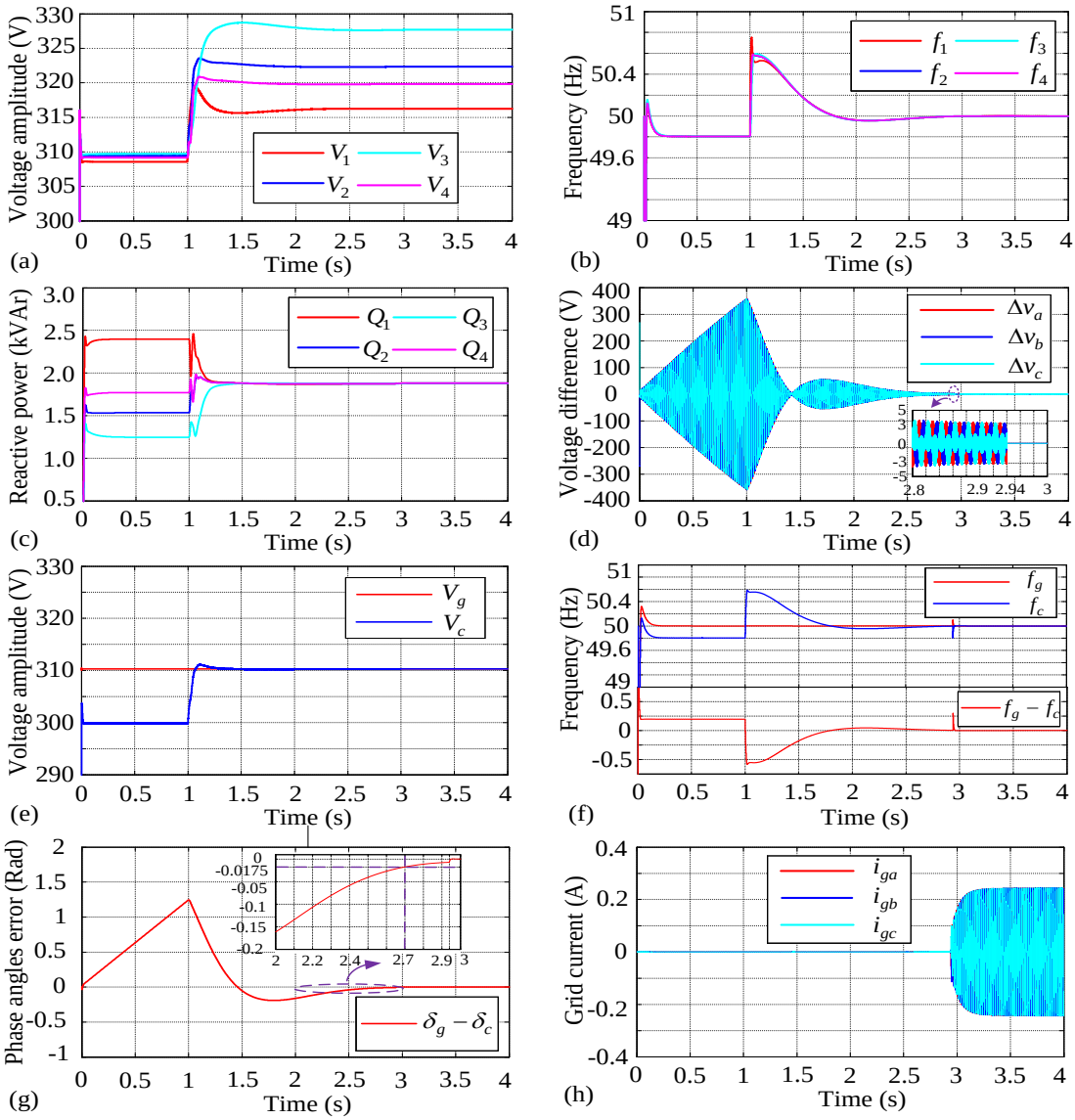

Fig. 11. Simulation results in scenario I: (a) voltage amplitudes of DGs, (b) frequencies of DGs, (c) output reactive powers of DGs, (d) voltage difference of grid and PCC, (e) voltage amplitudes of grid and PCC, (f) frequencies of grid and PCC voltage and their difference, (g) phase angle difference of grid and PCC voltage, (h) grid current.

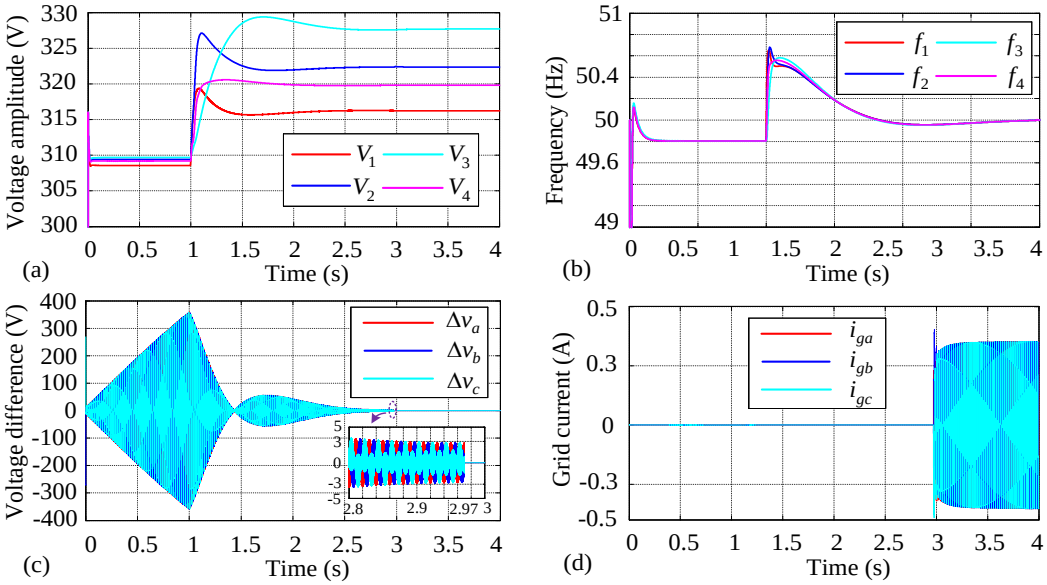

Fig. 12. Resiliency to failure in Link 2-3: (a) voltage amplitudes of DGs, (b) frequencies of DGs, (c) voltage difference of grid and PCC, and (d) grid current.

VIII. REFERENCES

[1] Khederzadeh M, Maleki H, Asgharian V, "Frequency control improvement of two adjacent microgrids in autonomous mode using back to back Voltage-Sourced Converters," International Journal of Electrical Power & Energy Systems, 2016, 74: 126-133.

[2] Sofla M A, Gharehpetian G B, "Dynamic performance enhancement of microgrids by advanced sliding mode controller," International Journal of Electrical Power & Energy Systems, 2011, 33(1): 1-7.

[3] H. Han, X. Hou, J. Yang, J. Wu, M. Su, and J. M. Guerrero, "Review of Power Sharing Control Strategies for Islanding Operation of AC Microgrids," IEEE Trans. Smart Grid, vol.7, no.1, pp.200-215, Jan.2016.

[4] J. C. Vasquez, J. M. Guerrero, and A. Luna, "Adaptive droop control applied to voltage-source inverters operating in grid-connected and islanded modes," IEEE Trans. Ind. Electron., vol.56, no.10, pp.4088-4096, Oct.2009.

[5] Giraldo J, Mojica-Nava E, Quijano N, "Synchronization of isolated microgrids with a communication infrastructure using energy storage systems," International Journal of Electrical Power & Energy Systems, 2014, 63: 71-82.

[6] M. N. Arafat, A. Elrayyah, and Y. Sozer, "An effective smooth transition control strategy using droop-based synchronization for parallel inverters," IEEE Trans. Ind. Appl., vol.51, no.3, pp.2443-2454, May/Jun, 2015.

[7] Moradi M H, Eskandari M, Hosseinian S M, "Cooperative control strategy of energy storage systems and micro sources for stabilizing microgrids in different operation modes," International Journal of Electrical Power & Energy Systems, 2016, 78: 390-400.

[8] M. Karimi-Ghartemani, "Universal integrated synchronization and control for single-phase DC/AC converters," IEEE Trans. Power Electron., vol.30, no.3, pp.1544-1557, Mar.2015.

[9] W. M. Strang, C. J. Mozina, B. Beckwith, T. R. Beckwith, S. Chhak, E. C. Fennell, E.W. Kalkstein, K. C. Kozminski, A. C. Pierce, P. W. Powell, D. W. Smaha, J. T. Uchiyama, S. M. Usman, and W. P. Waudby, "Generator synchronizing, industry survey results," IEEE Trans. Power Del., vol. 11,no. 1, pp.174-183, Jan. 1996.

[10] N. T. Stringer, "Voltage considerations during generator synchronizing," IEEE Trans. Ind. Appl., vol. 35, no. 3, pp. 526-529, May/Jun. 1999.

[11] N. W. A. Lidula and A. D. Rajapakse, "Voltage balancing and synchronization of microgrids with highly unbalanced loads,"Renewable and Sustainable Energy Reviews, vol.31, pp. 907-920, Jan.2014.

[12] J. C. Vasquez, J. M. Guerrero, M. Savaghebi, J. Eloy-Garcia, and R. Teodorescu, "Modeling, analysis, and design of stationary-reference-frame droop-controlled parallel three-phase voltage source inverters,"IEEE Trans. Ind. Electron., vol.60, no.4, pp.1271-1280, Apr.2013.

[13] C. Cho, J. Jeon, J. Kim, S. Kwon, K. Park, and S. Kim, "Active synchronizing control of a microgrid," IEEE Trans. Power Electron., vol. 26, no. 12, pp. 3707–3719, Dec. 2011.

[14] T. M. L. Assis and G. N. Taranto, "Automatic reconnection from intentional islanding based on remote sensing of voltage and frequency signals," IEEE Trans. Smart Grid, vol. 3, no. 4, pp. 1877-1884, Sep. 2012.

[15] A. Bellini, S. Bifaretti, and F. Giannini, "A robust synchronization method for centralized microgrids," IEEE Trans. Ind. Appl., vol.51, no.2, pp.1602-1609, Mar. /Apr., 2015.

[16] M. S. Golsorkhi, D. D. C. Lu, "A control method for inverter-based islanded microgrids based on V-I droop characteristics," IEEE Trans. Power Del., vol. 30, no. 3, pp. 1196–1204, Jun. 2015.

[17] J. M. Guerrero, M. Chandorkar, T-L. Lee, P. C. Loh, "Advanced control architectures for intelligent microgrids – part I: decentralized and hierarchical control," IEEE Trans. Ind. Electron., vol. 60, no. 4, pp. 1254-1262, Apr. 2013.

[18] R. Majumder, B. Chaudhuri, A. Ghosh, R. Majumder, G. Ledwich, F.Zare, "Improvement of stability and load sharing in an autonomous microgrid using supplementary droop control loop," IEEE Trans. Power sys., vol. 25, no. 2, pp. 796–808, May 2010.

[19] Q. C. Zhong, P.-L. Nguyen, Z. Ma, and W. Sheng, "Self-synchronized synchronverters: Inverters without a dedicated synchronization unit,"IEEE Trans. Power Electron., vol. 29, no. 2, pp. 617-630, Feb. 2014.

[20] S. S. Thale and V. Agarwal, "Controller area network assisted grid synchronization of a microgrid with renewable rnergy sources and storage," IEEE Trans. Smart Grid, to be published.

[21] A. Micallef, M. Apap, C. Spiteri-Staines, J. M. Guerrero, "Single-phase microgrid with seamless transition capabilities between modes of operation," IEEE Trans. Smart Grid, vol. 6, no. 6, pp. 2736–2745, Nov. 2015.

[22] Esmaeli A, "Stability analysis and control of microgrids by sliding mode control," International Journal of Electrical Power & Energy Systems, 2016, 78: 22-28.

[23] J. Giraldo, E. Mojica-Nava, N. Quijano, "Tracking of Kuramoto oscillators with input saturation and applications in smart grids," IEEE American Control Conference, 2014, pp. 2656-2661.

[24] J. Giraldo, E. Mojica-Nava, N. Quijano, "Synchronization of dynamical networks under sampling," European Control Conference (ECC), 2013, pp. 3839-3844.

[25] J. W. Simpson-Porco, F. Dorfler, and F. Bullo, "Synchronization and power sharing for droop-controlled inverters in islanded microgrids," Automatica, vol. 49, no. 9, pp. 2603–2611, 2013.

[26] F. Dörfler, J. W. Simpson-Porco, and F. Bullo, "Breaking the hierarchy: Distributed control & economic optimality in microgrids," IEEE Trans. Control Netw. Syst., to be published.

[27] A. Bidram A. Davoudi, F. K. Lewis, Z. Qu, "Secondary control of microgrids based on distributed cooperative control of multi-agent systems," IET Gener. Transm. & Distrib., vol. 7, no. 8, pp. 822-831, 2013.

[28] Q. Shafiee, J. M. Guerrero, and J. C. Vasquez, "Distributed secondary control for islanded microgrids - a novel approach," IEEE Trans. Power Electron., vol. 29, no. 2, pp. 1018–1031, 2014.

[29] F. Guo, C. Wen, J. Mao, and Y.-D. Song, "Distributed secondary voltage and frequency restoration control of droop-controlled inverter-based microgrids," IEEE Trans. Ind. Electron., vol. 62, no. 7, pp. 4355-4364, Jul. 2015.

[30] M. A. Mahmud, M. J. Hossain, H. R. Pota, A. M. T. Oo, "Improvement of stability and load sharing in an autonomous microgrid using supplementary droop control loop," IEEE Trans. Energy Conversion, vol. 29, no. 4, pp. 893–903, Dec. 2014.

[31] Liu W, Gu W, Xu Y, et al, "Improved average consensus algorithm based distributed cost optimization for loading shedding of autonomous microgrids," International Journal of Electrical Power & Energy Systems, 2015, 73: 89-96.

[32] Ospina A M, Quijano N, "Distributed control of small-scale power systems using noncooperative games," International Journal of Electrical Power & Energy Systems, 2016, 82: 535-544.

[33] J. Wei, D. Kundur, T. Zourntos, and K. Butler-Purry, "A flockingbased paradigm for hierarchical cyber-physical smart grid modeling and control," IEEE Trans. Smart Grid, vol. 5, no. 6, pp. 2687–2700, Nov. 2014.

[34] J. Wei, D. Kundur, and K. L. Butler-Purry, "A novel bio-inspired technique for rapid real-time generator coherency identification," IEEE Trans. on Smart Grid, vol. 6, pp. 178 – 188, January 2015.

[35] J. Wei, D. Kundur, "GOAliE: goal-seeking obstacle and collision evasion for resilient multicast routing in Smart Grid," IEEE Trans. Smart Grid, vol. 7, no. 2, pp. 567-579, Mar. 2016.

[36] C.-T. Lee, R.-P. Jiang, and P.-T. Cheng, "A grid synchronization method for droop-controlled distributed energy resource converters," IEEE Trans. Ind. Appl., vol. 49, no. 2, pp. 954–962, Mar./Apr. 2013.

[37] H. Behjati, A. Davoudi, and F. L. Lewis, "Modular DC-DC converters on graphs: Cooperative control," IEEE Trans. Power Electron., vol. 29, no.12, pp. 6725–6741, Dec. 2014.

[38] Z. Li, Z. Duan, G. Chen, and L. Huang, "Consensus of multiagent systems and synchronization of complex networks: A unified viewpoint," IEEE Trans. Circuits Sys. I: Reg. Papers, vol. 57, no. 1, pp. 213–224, Jan. 2010.

[39] X. Li, X. Wang, and G. Chen, "Pinning a complex dynamical network to its equilibrium," IEEE Trans. Circuits Syst. I: Reg. Papers, vol. 51, no. 10, pp. 2074–2087, Oct. 2004.

[40] J. Millman, "A useful network theorem,"Proc. of the IRE 28.9, 1940, pp. 413-417.

[41] IEEE Standard for Interconnecting distributed resources with electric power systems, IEEE Standard 1547, 2003, pp. 1–16.

[42] C. Cho, S.-K. Kim, J.-H. Jeon, and S. Kim, "New ideas for a soft synchronizer applied to CHP cogeneration," IEEE Trans. Power Del., vol. 26, no. 1, pp. 11–21, Jan. 2011.